한국해양공학회 2001년도 춘계학술대회 논문집 PP.254~259

트렌치내에서 복합 해저 관로 안정성의 수치해석과 실험해석 비교

조철희* · 신영섭** · 홍성근*** · ° 민경훈*** · 정광식***

Comparison of Numerical and Experimental Stability of Dual Subsea Pipeline in Trench

*Chul H. Jo** · *Young S. Shin*** · *Sung G. Hong**** · ° *Kyoung H. Min**** · *Kwang Sic Chung****

KEY WORDS. : dual pipeline, PIV, offshore pipeline stability

ABSTRACT : *There are advantages in the installation of dual subsea pipelines over two separate single lines. In many case it can reduce the cost for trench, back-filling and installation. However the installation of dual pipelines often requires technical challenges. Dual Pipelines should be placed to be stable to external loadings not only during the installation but also in the design life. Dual pipelines in trench can reduce the influence of external forces. To investigate applied forces as slope changes, number of experiments are conducted with PIV (Particle Image Velocimetry) in a circulating water channel. Numerical approaches are also made to compare with experimental results. The velocity fields around dual pipelines in trench are investigated and analysed. Comparison of both results show similar patterns of flow around dual pipelines. It is proved that the trench slope affects the pipeline stability significantly. The results can be applied in the stability design of dual pipelines in trench section. The complex flow patterns can be referenced effectively linked in the understanding of fluid around circular bodies in trench.*

1. INTRODUCTION

More than one pipe is required to be laid along the route on the seabed particularly in the development and operation of subsea satellite oil wells in many cases. For multiple pipe arrangements, it is difficult to determine the flow patterns around them and their effects by surrounding pipeline on the stability. (Rados and Pitt, 2000) To ensure a continuous operation of the system, adequate design criteria and considerations are required. (Knoll and Herbich, 1980).

Hydrodynamic loads on subsea pipeline resting on ocean bottom are a function of parameters associated with waves and currents acting around the pipeline. There have been numbers of studies conducted to develop a criteria to predict hydrodynamic loads imposed by external waves and currents. But not much for dual pipelines in trench section. Quite number of dual pipelines in many regions are placed in trench for protection from anchoring or fishing activities. However clear guidelines for the reduction of hydrodynamic loads of pipelines in trench are not provided except very limited arrangements and conditions. This research investigate the relationship between the hydrodynamic force at various slopes and flow velocity. A numerical study is conducted with Navier-Stokes and the continuity equations. Since trench geometries with dual pipes are very complex, grid shapes distributed near the intersection between pipes and trench are considered very important to obtain stable solutions. The elliptic transformation method is applied to get a smoothly distributed and clustered grid. The generalized spectral method which is

* 인하대학교 선박해양공학과 부교수
** 한라대학교 기계공학부 조교수
*** 인하대학교 선박해양공학과 대학원

applicable to general partial differential equations and boundary conditions is used to solve the pressure equation satisfying the continuity condition. It is well known that the oscillating lift and drag forces occur in the uniform flow around a circular body. Understanding this phenomenon, time advancements are proceeded until obtaining harmonically steady state. Number of physical models are installed and experimented at three current speeds with various trench section slopes in a circulating water channel. The flow patterns around dual cylinder models in trench are measured by the PIV system. Reduction coefficients for drag over various experimental cases are obtained.

2. THEORY

2.1 Numerical Analysis

The nondimensionalized equations for the conservation of mass and momentum for an incompressible viscous fluid are applied to develop the methods

Here, all can be written as ;

$$\frac{u^{n+1}}{\Delta t} = \frac{u^n}{\Delta t} + F^n - \frac{\partial p^n}{\partial x} \tag{1}$$

$$\frac{v^{n+1}}{\Delta t} = \frac{v^n}{\Delta t} + G^n - \frac{\partial p^n}{\partial y} \tag{2}$$

where F and G are defined as

$$F \equiv \frac{1}{R}\left(\frac{\partial^2 u}{\partial x^2} + \frac{\partial^2 u}{\partial y^2}\right) - u\frac{\partial u}{\partial x} - v\frac{\partial u}{\partial y} \tag{3}$$

$$G \equiv \frac{1}{R}\left(\frac{\partial^2 v}{\partial x^2} + \frac{\partial^2 v}{\partial y^2}\right) - u\frac{\partial v}{\partial x} - v\frac{\partial v}{\partial y} \tag{4}$$

The pressure equation may be expressed in the generalized coordinate form as follows:

$$\alpha p_{\xi\xi} - 2\beta p_{\xi\eta} + \gamma p_{\eta\eta} + \delta_p p_\xi + \delta_q p_\eta = \frac{D}{\Delta t} + \xi_x F_\xi + \eta_x F_\eta + \xi_y G_\xi + \eta_y G_\eta \tag{5}$$

where

$$\alpha = \nabla\xi \cdot \nabla\xi$$
$$\beta = -\nabla\xi \cdot \nabla\eta$$
$$\gamma = \nabla\eta \cdot \nabla\eta$$
$$\delta_p = \nabla^2\xi$$
$$\delta_q = \nabla^2\eta \tag{6}$$

The spectral method was used to solve Eq. (5). Eq. (5) may be rearranged as

$$\alpha_o p_{\xi\xi} - 2\beta_o p_{\xi\eta} + \gamma_o p_{\eta\eta} + \delta_{po} p_\xi + \delta_{qo} p_\eta = R$$
$$-(\alpha-\alpha_o)p_{\xi\xi} - (-2\beta+2\beta_o)p_{\xi\eta} - (\gamma-\gamma_o)p_{\eta\eta} - (\delta_p-\delta_{po})p_\xi - (\delta_q-\delta_{qo})p_\eta \tag{7}$$

where $\alpha_o, \ldots, \delta_{qo}$ are mean coefficients of $\alpha, \ldots, \delta_q$ in the ξ direction respectively. The pressure may be expanded in Fourier series in the ξ direction as follows:

$$p_{\xi\xi} = p_k(\eta) e^{ik\xi} \tag{8}$$

Then p_ξ and p can be obtained by integrating Eq. (8) as follows:

$$p_\xi = \frac{p_k(\eta)}{ik} e^{ik\xi} + p_o(\eta)\xi + a(\eta) \tag{9}$$

$$p = \frac{p_k(\eta)}{(ik)^2} e^{ik\xi} + \frac{1}{2} p_o(\eta)\ \xi^2 + a(\eta)\xi + b(\eta) \tag{10}$$

By substituting Eqs. (8), (9) and (10) into Eq. (7), the ordinary differential equation may be derived as

$$\left[\frac{\gamma_o(\eta)}{(ik)^2}\ddot{p}_k(\eta) + \left\{\frac{-2\beta_o(\eta)}{ik} + \frac{\delta_{qo}(\eta)}{(ik)^2}\right\}\dot{p}_k(\eta) + \left\{\alpha_o(\eta) + \frac{\delta_{po}(\eta)}{ik}\right\}p_k(\eta)\right]e^{ik\xi}$$
$$+\frac{\gamma_o}{2}(\eta)\xi^2\ddot{p}_o(\eta) + \left\{-2\beta_o(\eta)\xi + \frac{\delta_{qo}(\eta)}{2}\xi^2\right\}\dot{p}_o(\eta) + \delta_{po}(\eta)\xi p_o(\eta)$$
$$+\gamma_o(\eta)\xi\ddot{a}(\eta) + \{-2\beta_o(\eta) + \delta_{qo}(\eta)\xi\}\dot{a}(\eta) + \delta_{po}(\eta)a(\eta)$$
$$+\gamma_o(\eta)\ddot{b}(\eta) + \delta_{qo}(\eta)\dot{b}(\eta)$$
$$= \overline{R}(\xi, \eta) \tag{11}$$

where

$$\overline{R} = R - (\alpha-\alpha_o)p_{\xi\xi} - (-2\beta+2\beta_o)p_{\xi\eta} - (\gamma-\gamma_o)p_{\eta\eta} - (\delta_p-\delta_{po})p_\xi - (\delta_q-\delta_{qo})p_\eta \tag{12}$$

Eq. (8) may be written in each spectral mode as follows:

$$\frac{\gamma_o(\eta)}{(ik)^2}\ddot{p}_k(\eta) + \left\{\frac{-2\beta_o(\eta)}{ik} + \frac{\delta_{qo}(\eta)}{(ik)^2}\right\}\dot{p}_k(\eta) + \left\{\alpha_o(\eta) + \frac{\delta_{po}(\eta)}{ik}\right\}p_k(\eta) = \overline{M_k}(\eta) \quad , k=1,2\ldots, \tag{13}$$

$$\gamma_o(\eta)\ddot{b}(\eta) + \delta_{qo}(\eta)\dot{b}(\eta) = \overline{M_o}(\eta) \tag{14}$$

where $\overline{M_k}(\eta)$ is the m^{th} spectral mode of $\overline{M}(\xi, \eta)$ and

$$\overline{M}(\xi, \eta) = \overline{R}(\xi, \eta) - \frac{\gamma_o}{2}(\eta)\xi^2\ddot{p}_o(\eta) - \left\{-2\beta_o(\eta)\xi + \frac{\delta_{qo}(\eta)}{2}\xi^2\right\}\dot{p}_o(\eta) - \{\alpha_o(\eta) + \delta_{po}(\eta)\xi\}p_o(\eta)$$

$$-\gamma_o(\eta)\xi\dot{a}(\eta)-\{-2\beta_o(\eta)-\delta_{qo}(\eta)\xi\}\dot{a}(\eta)-\delta_{po}(\eta)a(\eta) \quad (15)$$

From the boundary condition at the ξ ends, $p_o(\eta)$ and $a(\eta)$ may be obtained as,

$$p_o(\eta)=\frac{\dot{p}(\xi_1,\eta)-\dot{p}(\xi_2,\eta)}{\xi_1-\xi_2} \quad (16)$$

$$a(\eta)=\frac{p(\xi_1,\eta)-p(\xi_2,\eta)}{\xi_1-\xi_2}-\frac{\xi_1+\xi_2}{2}p_o(\eta) \quad (17)$$

Eq. (7) are solved iteratively to obtain convergent pressure fields.

2.2 Applied Theory

The schematic diagram of Fig. 1 represents a configuration of dual pipes in open trench. Dual pipelines in open trench is subjected to external loads such as wave and current (Sumer and Jorgen, 1997).

The drag force in trench can be estimated with reduction coefficients which vary with trench depth (H) and slope. The relating equations are as described below (Jo and et. al., 2000):

$$F^*_{Dn} = F_D \times RF_{Dn} \quad (18)$$

where

F^*_{Dn} : drag force per unit length in open trench on individual pipeline
RF_{Dn} : reduction coefficient on drag force on individual pipeline
F_D : drag force per unit length on sea bottom

The reduction coefficients are dependent on velocity reduction factor and Reynolds number. The velocity reduction factor can be obtained from the measurement of velocity both on seabed and in trench. The velocity reduction factor can be derived from (19):

$$\beta_n = \frac{u^*_{en}}{u_e} \quad (19)$$

where

β_n : reduction factor on velocity for individual pipeline
u_e : effective velocity of flow on sea bottom
u^*_{en} : effective velocity of flow in open trench for individual pipeline

As per the velocity reduction factor, the drag forces and reduction coefficients in trench can be written as follows:

$$RF_{Dn} = \frac{F^*_{Dn}}{F_D} = \frac{C^*_{Dn}}{C_D}\beta_n^2 \quad (20)$$

where,

C_{Dn}^* : coefficient of drag force in open trench for individual pipeline
C_D : coefficient of drag force on sea bottom

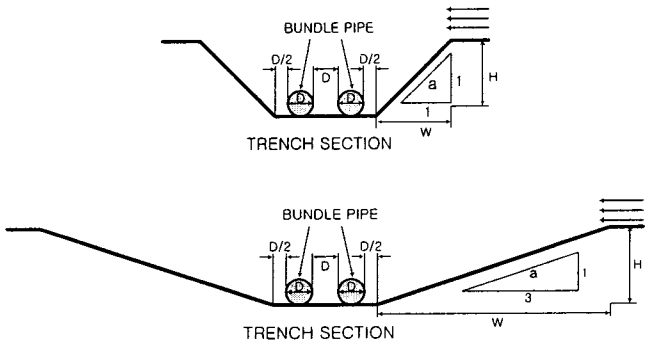

Fig. 1 Schematic diagram of dual pipelines in trench

3. MODELING

3.1 Modeling of Numerical Method

A grid is generated by application of the elliptic transformation (Steger and Sorenson, 1979). Fig. 2 shows the generated grid around the dual pipes in trench. The uniform flow is used as the initial condition. No slip condition is used at the trench bottom and pipes. The periodic boundary conditions are applied at inflow and downstream boundaries. Time increments are taken sufficiently small to satisfy C.F.L. condition.

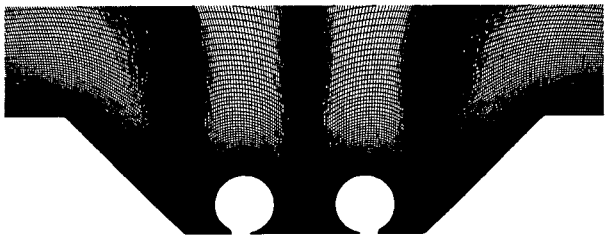

Fig. 2 Schematic diagram of grid generation

3.2 Modeling of Experimental Method

A schematic diagram of experimental arrangement of dual pipes in a trench is shown in Fig. 1 where D and H stand for outside diameter and trench depth, respectively. The space of dual pipes is fixed at D where D is the diameter of pipe. The pipes are placed from the end of trench at the distance of D/2. The frames for the trench section are made out of bronze, and the seabed of transparent flexi-glass of 5 mm thickness. The experiments are conducted in a circulating water tunnel at various current speeds. The test section of the water tunnel is 3.5m long, and has a cross section of 1.2m (width) and 0.9m (height) and water depth of 0.7m.

3.3 P.I.V. System

To identify velocity fields in the trench with various slopes, the P.I.V. measurements are performed with an optical setup illustrated in Fig. 3. To provide the trench with two-dimensional sheet of light in the symmetric plane, a 1.0W Ar-ion laser is supplied to the flow field through a fiber optic cable together with a cylindrical lens. The particles of 150-200 μm diameter having about same density with water are seeded in the tunnel after static electricity is suppressed. The visual images are captured by a CCD (Charge Coupled Device) camera (SONY-XC77RR) and stored on a tape via a video recorder. The captured images controlled by AOM are sent to odd and even fields and processed in an image board (DT3155, 640480 pixels) of a host computer (250MHz CPU).

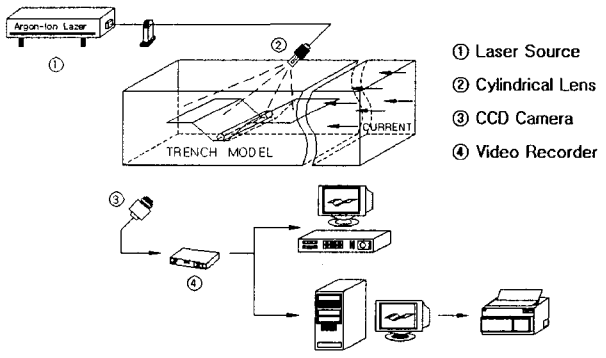

Fig. 3 Experimental arrangement

4. RESULT AND DISCUSSION

From the experiment and numerical analyses, the velocity fields around the circular bodies in various trench sections are obtained. From these data, velocity reduction factors and drag reduction coefficients are investigated. Should it be 0.5, it means that the hydrodynamic force on a body is half over that on the seabed. As cylindrical pipes are placed in a trench, both the drag and the lift forces are reduced considerably depending on the position of the pipes in trench. This is due to the sheltering effect by the trench. It was reported that even in the same trench depth a steeper slope results in a higher reduction effect in terms of pipeline stability.

The parameters of geometrical importance may be listed as the slope length (W), trench depth (H), cylinder diameter (D). Two non-dimensional parameters are determined by H/D, and W/H. To investigate the current effect on the drag force, the case of 0.2 m/s , 0.3 m/s and 0.4 m/s are selected. The models having H/D of 2, 4, and W/H = 1, 3 are used. The identical conditions are also applied in the numerical approach to compare with the experimental results.

4.1 Flow Pattern in Trench

The computed and measured mean velocity vectors around dual pipes in various trench configurations are compared. For the case of H/D=2 and W/H= 1 with current velocity 0.2 m/s, the flow fields are presented in Fig. 4. The separated shear-layer in the fore part of the trench produces several vortex motions.

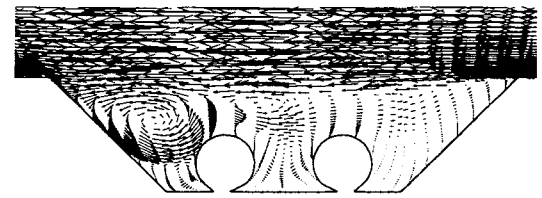

(a) Computed (W/H=1 , H/D=2)

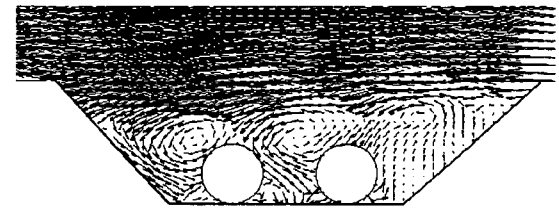

(b) Measured (W/H=1 , H/D=2)

Fig. 4 Compared mean-velocity patterns (current velocity is 0.2 m/s)

4.2 Drag Coefficient for Difference Slopes

The drag reduction coefficients for various trench slopes are as shown in Fig. 5. Figures indicate that as the slope increases the reduction factor decrease. The

results show that the reduction factors and coefficients for slope W/H=3 is much larger than those for slope W/H=1. When W/H=1, there are not much of differences in the drag reduction factor between upstream and downstream of pipes. But the drag reduction factor of upstream pipe is much larger than downstream one when W/H=3. This trends are revealed very similar between measured and computed results. However, it seems that the slope influences significantly to the reduction factors.

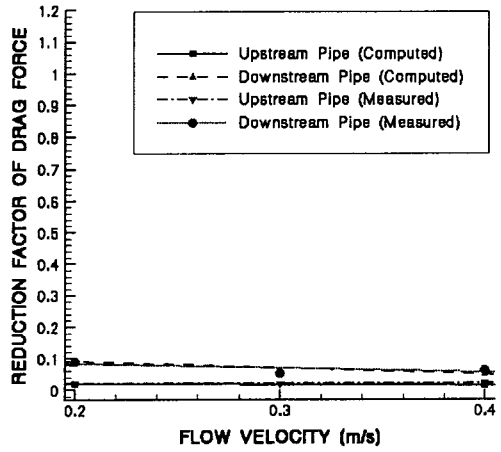

(a) W/H = 1

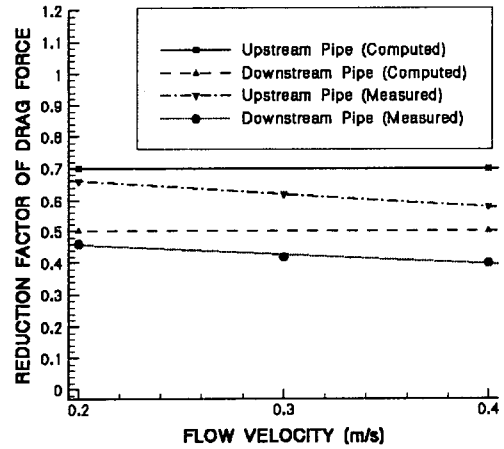

(b) W/H = 3

Fig. 5 Drag force reduction factor vs. trench slope (H/D=2)

4.3 Drag Coefficient for Upstream and Downstream

The drag reduction factors for upstream and downstream around dual pipes are shown in Fig. 6. They indicate that the drag reduction factor of upstream pipe are smaller than downstream when W/H=1. On the contrary, the drag reduction factor of upstream pipe is larger than downstream when W/H=3 for computed and measured results. They show similar tendency in the both results for various flow velocities.

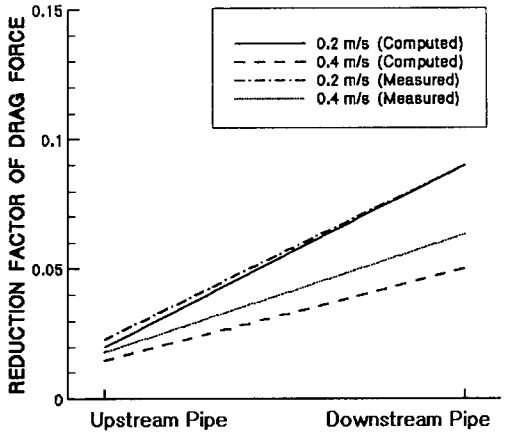

(a) W/H = 1

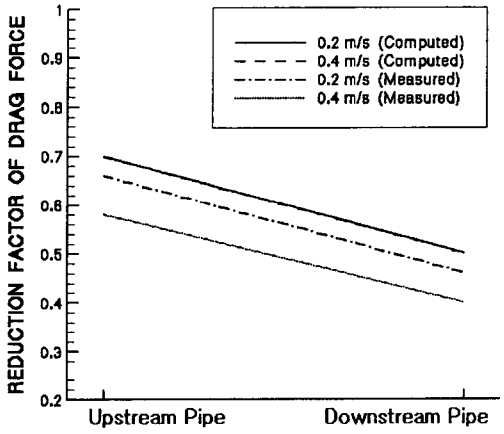

(b) W/H = 3

Fig. 6 Drag force reduction factor for upstream and downstream (H/D=4)

5. CONCLUSION

The reduction factors for dual pipes in various trench slopes at different Reynolds numbers are investigated with an application of PIV system. From numerical and experimental studies, the followings are observed:

1. The trench slope greatly influence on reduction factors. The slope W/H=1 shows significant effect in reducing the reduction factor. As the trench slope increases reduction factors remarkably becomes smaller.
2. The drag force acting on the downstream of pipe is not always smaller than the upstream. For example, a larger drag force is noticed on the downstream of pipe

when W/H=1

This study can contribute in the understanding of oscillating drag characteristics and reduction factors around dual pipes in various trench slopes.

REFERENCE

Jo C. H., Kim K .S. and Hong S. G. (2000), "Subsea Pipeline in Various Trench Sections", International Offshore and Polar Engineering Conference, Vol II, pp. 218-225

Knolll, D. A. and Herbich, J. B. (1980), "Wave and current forces on a submerged offshore pipeline", Offshore Technology Conference, pp. 227-234

Rados K. G. and Pitt D. (2000), "On the Interaction of Pipe Lines on the Seabed", International Offshore and Polar Engineering Conference, Vol II, pp. 155-161

Steger J. L. and Sorenson R. L. (1979), "Automatic mesh-point clustering near a boundary in grid generation with elliptic partial differential equations", Journal of computational physics 33, pp. 405-410

Sumer, B. M. and Jorgen Fredsoe (1997), "Hydrodynamics around circular structures", World Scientific Publishing Co. Pte. Ltd.